Magnetic anisotropy in cyano-bridged bimetallic ferromagnets synthesized from the $[Mo(CN)_7]^{4-}$ precursor

Olivier Kahn,[a] Joulia Larionova[a] and Lahcène Ouahab[b]

[a] *Laboratoire des Sciences Moléculaires, Institut de Chimie de la Matière Condensée de Bordeaux, UPR CNRS No 9048, 33608 Pessac, France. E-mail: kahn@icmcb.u-bordeaux.fr*

[b] *Laboratoire de Chimie du Solide et Inorganique Moléculaire, UMR CNRS No 6511, Université de Rennes I, 350042 Rennes, France*

Received (in Cambridge, UK) 6th January 1999, Accepted 9th March 1999

The goal of this feature article is to introduce the dimension 'magnetic anisotropy' in the field of molecule-based magnets. For that, we have focused on three cyano-bridged $Mn^{II}Mo^{III}$ compounds synthesized from the $[Mo^{III}(CN)_7]^{4-}$ precursor. The pentagonal bipyramid structure of this precursor is not compatible with a cubic lattice, as found in the Prussian blue phases. In this precursor, Mo^{III} has a low-spin configuration, with a local spin $S_{Mo} = 1/2$, and a strongly anisotropic *g* tensor. Two of the compounds have a three-dimensional structure. Their formulas are $Mn_2(H_2O)_5Mo(CN)_7 \cdot nH_2O$, with $n = 4$ for the α phase, and $n = 4.75$ for the β phase. One of the compounds, of formula $K_2Mn_3(H_2O)_6[Mo(CN)_7]_2 \cdot 6H_2O$, has a two-dimensional structure, with K^+ cations and water molecules located between double-sheet layers. The compounds crystallize in the monoclinic system, and the lattice symmetries are very low. For the three compounds, we have succeeded in growing well shaped single crystals suitable for magnetic anisotropy measurements, and we have investigated the magnetic properties as follows: first, we have determined the magnetic axes by looking for the extremes of the magnetization in the three crystallographic planes *ab*, *bc*, and *ac*. Then, we have measured the temperature and field dependences of the magnetization in the dc mode along the three magnetic axes. These measurements have revealed the existence of several magnetically ordered phases for the three-dimensional compounds, and of field-induced spin reorientations for the three compounds. For the very first time in the field of molecular magnetism, we have been able to determine the magnetic phase diagram for each compound. We have obtained additional information from magnetic data recorded in the ac mode, with both zero and non-zero static fields. Finally, we have found that when the non-coordinated water molecules are released, the long-range magnetic ordering temperatures are shifted toward higher temperatures. Irrespective of the structural details, the Mo^{III}–C–N–Mn^{II} interaction has been found to be ferromagnetic. We have discussed this unexpected result, and proposed a mechanism accounting for this. We have also discussed the factors governing the magnetic anisotropy of the compounds.

Introduction

The first two molecular compounds exhibiting a spontaneous magnetization below a certain critical temperature, T_c, were described in 1986.[1,2] These reports have opened a new field of research, that of molecule-based magnets, and in the last decade quite a few new compounds of that kind have been synthesized.[3–19] What characterizes this field of research is its deeply multidisciplinary nature; it brings together synthetic organic, organometallic, and inorganic chemists along with theoreticians and physicists as well as material and life science people.

To a large extent, the field so far has been governed by the race toward high coercivity and/or high critical temperature. High coercivity means that the material has a pronounced memory effect. As a matter of fact, applying a weak magnetic field to a magnet results in a saturation magnetization aligned in the field direction. When the field is switched of, the magnetization does not disappear, but takes a value called remnant magnetization. The coercive field is the field which must be applied in the opposite direction to annul this remnant magnetization, *i.e.* to suppress the information associated with the remnant magnetization. Recently, a very hard molecule-based magnet was discovered. Its coercive field depends on the particle size; it may be as large as 25 kOe at 5 K. This compound contains three kinds of spin carriers, Co^{2+} and Cu^{2+} ions as well as radical cations. It structure is very peculiar; it consists of two perpendicular honeycomb like (or graphite like) networks which interpenetrate in such a way that each hexagon belonging to one of the networks is interlocked with a hexagon belonging to the perpendicular network.[20–22] The key factor of the huge coercivity is the presence of very anisotropic Co^{2+} ions in octahedral surroundings. The interlocking of the two networks also contributes to this coercivity.

High critical temperature obviously means that the magnetically ordered state is easily accessible. In that respect, T_c above room temperature is a must. This goal has been reached with a compound of formula $V^{II}_{0.42}V^{III}_{0.58}[Cr^{III}(CN)_6]_{0.86} \cdot 2.8H_2O$.[23] This compound belongs to the vast family of the Prussian blue like phases with the general formula $A_k[B(CN)_6]_l \cdot nH_2O$ where

Olivier Kahn was born in Paris (France). He received his PhD thesis from the University of Paris in 1969. He became Professor of Chemistry at the University of Paris South in 1975, and moved to the Institut de Chimie de la Matière Condensée de Bordeaux in 1995. He is presently Professor at the University of Bordeaux I, and Member of the Institut Universitaire de France. Olivier Kahn is a Fellow of the (French) Academy of Science and of other academies. His fields of research are molecular materials, molecular electronics, and molecular magnetism.

Joulia Larionova was born in Saint Petersburg (Russia). She received her PhD thesis from the University of Bordeaux I in 1998. She initiated the work on the anisotropy properties of molecule-based magnets and determined the first magnetic phase diagrams for this class of compounds during her PhD.

Lahcène Ouahab was born in Sétif (Algeria). He received his PhD thesis from the University of Rennes I in 1985. He is presently Director of Research at the Laboratoire de Chimie du Solide et Inorganique Moléculaire of the University of Rennes I, and leads the molecular materials group. His fields of research concern the synthesis, and the crystal chemistry of molecular materials, in particular charge transfer complexes, radical ion salts, and organic–inorganic hybrids.

A is a high spin metal ion and B a low spin one. The basic structure is faced-centered cubic with A–N–C–B linear linkages along three perpendicular directions. Alkaline cations may occupy A_4 or B_4 tetrahedral sites. For $k > 1$, some $B(CN)_6$ groups are missing, which creates a local breaking of the three-dimensional periodicity. These vacant sites are usually occupied by water molecules coordinated to the adjacent A site.[24,25] The magnetic interaction between nearest neighbor A and B ions may be antiferro- or ferromagnetic. In the former case, the local spins tend to align in an antiparallel way. When it is so, the compound below T_c is a ferrimagnet, provided that there is no exact cancellation of the A and B spin sublattices. This situation is by far the most frequent. In the latter case, the local spins tend to align in a parallel way, and below T_c the compound is a ferromagnet. One of the appealing aspects of the magnetic studies dealing with Prussian blue phases[26–30] resides in the fact that it is possible to predict the nature, and to estimate *a priori* the value of the critical temperature, using simple theoretical models based on the symmetry of the singly occupied orbitals.[31] This is due to the fact that the symmetry of both the A and B metal sites is strictly octahedral so that the e_g and t_{2g} orbitals do not mix. The design of the room temperature magnet mentioned above does not arise from serendipity, but was achieved in a rational way.[32] The cubic symmetry of the Prussian blue phases, however, has a cost. These compounds are structurally, and hence magnetically isotropic, and many interesting features associated with the structural and magnetic anisotropies cannot be observed. It may be noticed that nobody so far has succeeded in growing single crystals of Prussian blue phases suitable for detailed magnetic measurements. This situation is not too embarrassing as no anisotropy is expected, except perhaps a weak shape anisotropy for thin film samples. On the other hand, the thorough investigation of the properties of molecule-based magnets of low symmetry requires obviously well shaped single crystals.

The goal of this article is to emphasize the beauty and the richness of the phenomena arising from the low symmetry of molecule-based magnets. For that, we will focus on cyano-bridged bimetallic magnets synthesized from the $[Mo(CN)_7]^{4-}$ precursor. The choice of this precursor is motivated by three reasons: (i) as for the Prussian blue phases, the presence of cyano ligands can lead to extended lattices. (ii) These networks should be of low symmetry; as a matter of fact, the heptacoordination of the precursor is not compatible with a cubic symmetry. (iii) In $KNa_2[Mo(CN)_7]\cdot 2H_2O$, the Mo^{III} ion is in a low-spin pentagonal bipyramid environment. The orbitally degenerate ground state, $^2E''_1$, is split into two Kramers doublets by the spin–orbit coupling, and the ground Kramers doublet is strongly anisotropic.[33–35] In other words, the value of the magnetization when applying a magnetic field strongly depends on the orientation of this field with respect to the fivefold axis of the pentagonal bipyramid.

We will try to present this article in a tutorial way; we will report on the magnetic properties of three compounds, but each new concept in molecular magnetism will be introduced and discussed only once.

The three-dimensional compounds $Mn_2(H_2O)_5Mo(CN)_7\cdot nH_2O$, α and β phases

Crystal structure of the α phase

The slow diffusion of two aqueous solutions containing $K_4[Mo(CN)_7]\cdot 2H_2O$ and $[Mn(H_2O)_6](NO_3)_2$, respectively, affords two kinds of single crystals, with elongated plate (α phase) and prism (β phase) shapes.[36,37] The local environments of the metal sites are similar for both phases, but the three-dimensional organizations are different. There is one molybdenum site along with two manganese sites, denoted as Mn1 and Mn2, as shown in Fig. 1. The molybdenum atom is surrounded by seven –C–N–Mn linkages, four of them involving a Mn1 site and three of them a Mn2 site. The geometry may be described as a slightly distorted pentagonal bipyramid. Both Mn1 and Mn2 sites are in distorted octahedral surroundings. Mn1 is surrounded by four –N–C–Mo linkages and two water molecules in *cis* conformation. Mn2 is surrounded by three −N–C–Mo linkages and three water molecules in a *mer* conformation. The three-dimensional organization for the α phase may be described as follows: edge-sharing lozenge motifs $(MoCNMn1NC)_2$ form bent ladders running along the *a* direction. Each ladder is linked to four other ladders of the same kind along the [011] and [01 − 1] directions through cyano bridges. These ladders are further connected by the $Mn2(CN)_3(H_2O)_3$ groups. Mn2 is linked to a Mo site of one of the ladders and to two Mo sites of the adjacent ladder. The structure as a whole viewed along the *a* direction is represented in Fig. 2.

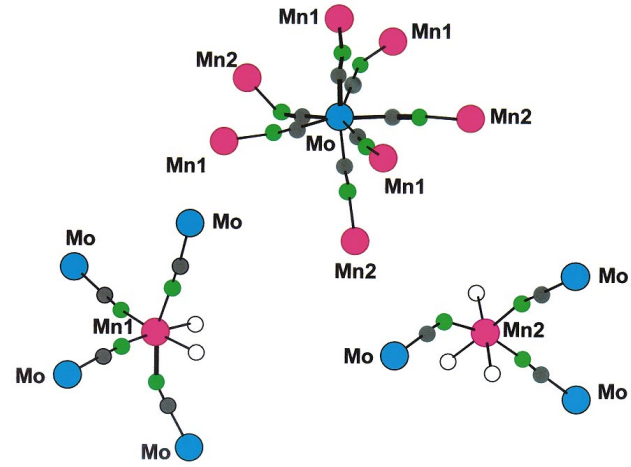

Fig. 1 Local structure of the molybdenum and manganese sites for $Mn_2(H_2O)_5Mo(CN)_7\cdot 4H_2O$ (α phase). The color code is the following: the manganese atoms are in red, the molybdenum atoms in blue, the carbon atoms in black, the nitrogen atoms in green, and the oxygen atoms (of water molecules) in white.

Magnetic properties of the α phase

We first checked that in the three crystallographic planes *ab*, *bc*, and *ac*, the extremes of the magnetization are obtained when the field is aligned along the *a*, *b* and *c** axes. Therefore, these axes are the magnetic axes of the compound. It may be noticed that the twofold axis of the monoclinic lattice, *b*, was necessarily one of the magnetic axes.[38] All the magnetic measurements were carried out on single crystals with the external field successively applied along these three axes. We first measured the temperature dependences of the magnetization, *M*, under a field of 5 Oe. The three curves are shown in Fig. 3. They reveal that the material is anisotropic, the magnetization along the easy magnetization axis, *b*, being about twice as large as along the *a* axis. Moreover, these curves exhibit a break with an inflexion point at $T_{1c} = 51$ K along with another anomaly, more visible along the *a* axis, at $T_{2c} = 43$ K. Very few magnetic anisotropy measurements on molecule-based magnets were performed so far.[3,39]

The most accurate technique to determine transition temperatures is the measure of the heat capacity as a function of temperature. In the present case, the heat capacity curve shows a λ peak at 51 K, but nothing is detected at 43 K (see Fig. 4). It follows that the compound presents two magnetic transitions, and the entropy change associated with that occurring at 51 K is much larger than the entropy change associated with that occurring at 43 K.

In order to obtain more insights on the magnetic anomaly detected at 43 K, visible essentially along the *a* direction, we measured the magnetization along this direction with an external field varying from 1 up to 100 Oe. The results are

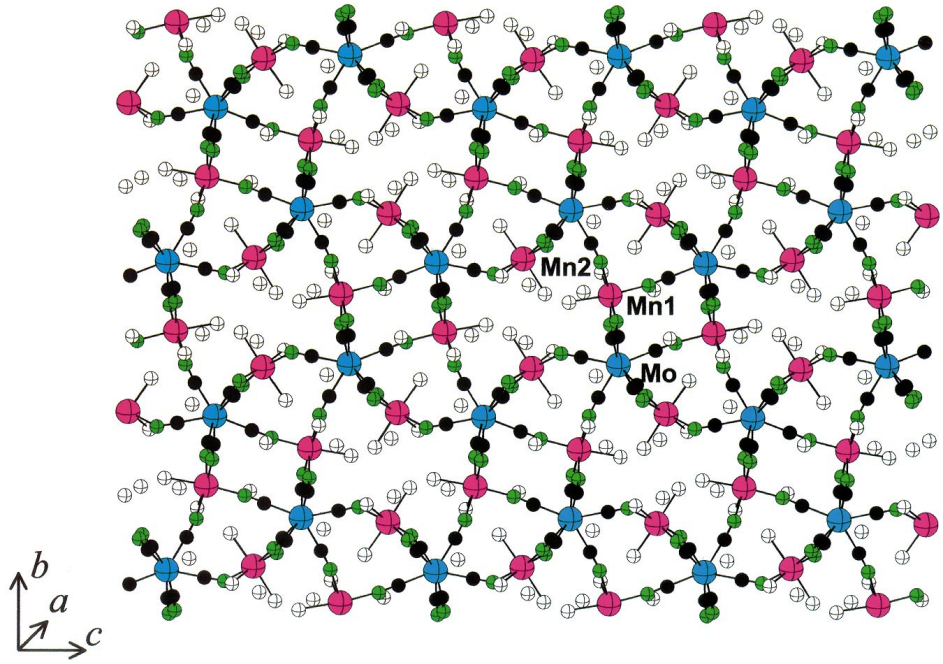

Fig. 2 Structure of the compound $Mn_2(H_2O)_5Mo(CN)_7{\cdot}4H_2O$ (α phase) viewed along the *a* direction.

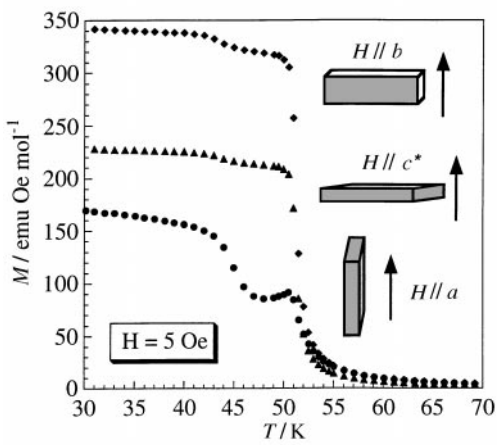

Fig. 3 Temperature dependences of the magnetization along the *a*, *b* and *c** directions, using an external field of 5 Oe, for $Mn_2(H_2O)_5Mo(CN)_7{\cdot}4H_2O$ (α phase).

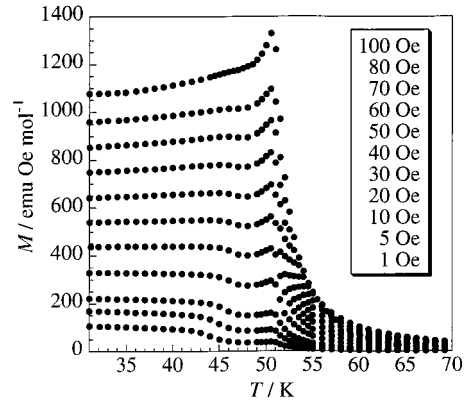

Fig. 5 Temperature dependences of the magnetization along the *a* direction, using different values of the external field, for $Mn_2(H_2O)_5Mo(CN)_7{\cdot}4H_2O$ (α phase).

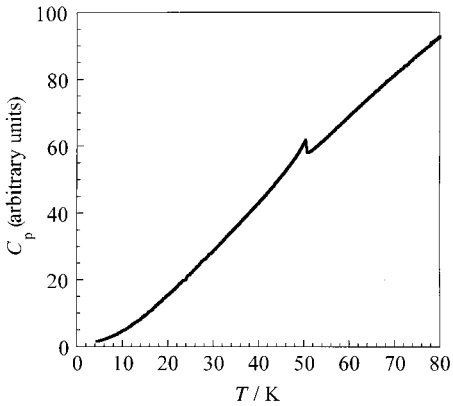

Fig. 4 Temperature dependence of the heat capacity for $Mn_2(H_2O)_5Mo(CN)_7{\cdot}4H_2O$ (α phase).

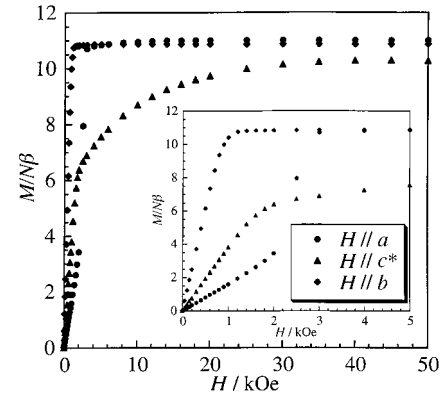

Fig. 6 Field dependences of the magnetization at 5 K along the *a*, *b* and *c** directions for $Mn_2(H_2O)_5Mo(CN)_7{\cdot}4H_2O$ (α phase).

displayed in Fig. 5. T_{2c} is shifted toward higher temperatures as the magnetic field increases, and eventually, for a field of *ca.* 100 Oe, merges with the transition at 51 K. For each field, T_{2c} was determined as the inflexion point of the $M = f(T)$ curve.

We then measured the field dependences of the magnetization at 5 K along the *a*, *b* and *c** directions (see Fig. 6). The curves are strictly identical when increasing and decreasing the field; the compound exhibits no coercivity. Along the easy magnetization direction, *b*, the saturation is reached with *ca.* 1 kOe. The saturation magnetization is found equal to 11 Nβ. This value corresponds exactly to what is expected for one $S_{Mo} = 1/2$ and two $S_{Mn} = 5/2$ local spins aligned along this direction. The interaction between adjacent Mo^{III} and Mn^{II} ions is ferromagnetic. Along the *c** direction, the magnetization increases progressively when applying the field, and even at 50 kOe the

saturation is not totally reached. Along the *a* direction, the *M versus H* curve is peculiar; it shows an inflexion point for a critical field, H_c, of about 2.2 kOe. We are faced with a field-induced spin reorientation phenomenon.[40–44]

Field-induced spin reorientation

Let us examine in more detail what happens when applying the field along the *a* axis. In zero field, the resulting moment of 11 Nβ is essentially aligned along *b*. When applying the field, first this moment hardly rotates from *b* to *a*, then for a critical value of the field the rotation becomes much easier. Finally, for a saturation value of the field, H_{sat}, the moment is aligned along *a*. The spin reorientation is a non-linear phenomenon. It is difficult to unhook the moment from the *b* axis. When the field is large enough, this unhooking is realized, and then a weak increase of the field induces a strong rotation until the moment is collinear with *a*. To determine the H_c and H_{sat} *versus T* curves, we measured the field dependence of the magnetization along *a* every 5 K in the 5–51 K range. The critical field at each temperature was determined as the field for which the d*M*/d*H* derivative is maximum. The saturation field at each temperature was determined as the weakest field for which the saturation is reached. The temperature dependences of H_c and H_{sat} for a field applied along the *a* axis are utilized to determine the magnetic phase diagram of the compound.

Magnetic phase diagram

From the magnetic data presented above, it is possible to plot the magnetic phase diagram of the compound when the field is applied along the *a* axis. This diagram shown in Fig. 7 presents

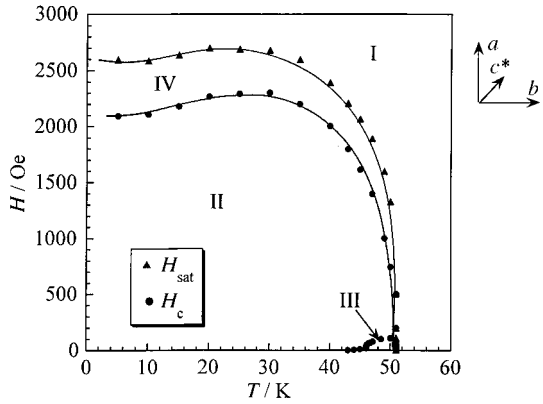

Fig. 7 Magnetic phase diagram for $Mn_2(H_2O)_5Mo(CN)_7{\cdot}4H_2O$ (α phase); the full lines are a guide to the eye.

four domains. Domain I is the paramagnetic domain in which the spins are either randomly oriented, or aligned along the field direction. Domains II and III are ferromagnetic domains in which the spins are essentially aligned along the *b* direction. Domain III is limited to the 43–51 K temperature range and the 0–100 Oe field range. Domain IV, finally, is limited by the $H_c = f(T)$ and $H_{sat} = f(T)$ curves, and corresponds to a mixed domain in which the spins may rotate easily from the *b* to the *a* direction. It is worth mentioning that the boundary between domains II and IV corresponds to a first-order transition, while that between domains I and IV corresponds to a second-order transition.

The question we are faced with is the difference between domains II and III. We have seen that the entropy variation associated with the transition between these two domains is very weak, and not detected in the heat capacity curve of Fig. 4. Therefore, the magnetic structures of these domains are similar to each other. The transition between these two domains, at 43 K in zero field, is more pronounced when applying the field along the *a* axis than along the other two magnetic axes. This strongly suggests that the main difference between domains II and III concerns the component of the resulting moment along *a*. Assuming that the magnetic symmetry of the low-temperature domain II is lower than that of the high-temperature domain III, we may suggest that domain III is a perfectly ferromagnetic domain with the magnetic moments aligned along *b* in zero field, and that a small canting occurs as *T* is lowered below 43 K, with a weak component of the resulting moment along *a*. If it was so, applying a field of 100 Oe along *a* would destabilize the perfectly ferromagnetic domain in favor of the weakly canted domain. Alternatively, the two domains might be weakly canted, with a component of the moment along *a*, the degree of canting being slightly more pronounced in domain II. Neutron diffraction studies should allow us to specify the differences between domains II and III.

A quick look on the β phase

The structure of the β phase is shown in Fig. 8. Each ladder made of edge-sharing lozenge motifs is surrounded only by two instead of four identical ladders. This phase again exhibits a ferromagnetic transition at T_c = 51 K. It is even more anisotropic than the α phase, and the magnetic phase diagram is even more complex, with several ferromagnetically ordered domains, and a spin reorientation domain.[45]

The partial dehydration of the α or β phase leads to the same compound which exhibits a long-range ferromagnetic ordering at 66 K along with a coercive field of 850 Oe at 5 K.

The two-dimensional compound $K_2Mn_3(H_2O)_6[Mo(CN)_7]_2{\cdot}6H_2O$

When the slow diffusion between aqueous solutions containing $K_4[Mo(CN)_7]{\cdot}2H_2O$ and $[Mn(H_2O)_6](NO_3)_2$, respectively, takes place in the presence of an excess of K^+ ions, a two-dimensional compound of formula $K_2Mn_3(H_2O)_6$-$[Mo(CN)_7]_2{\cdot}6H_2O$ is obtained.[46] The structure contains again a unique molybdenum site along with two manganese sites, denoted as Mn1 and Mn2, as shown in Fig. 9. The molybdenum atom is surrounded by six –C–N–Mn linkages and a terminal –C–N ligand. The geometry may be described as a strongly distorted pentagonal bipyramid, and both the Mo–C–N and C–N–Mn bridging angles deviate significantly from 180°. Both the Mn1 and Mn2 sites are surrounded by four –N–C–Mo linkages and two water molecules in *trans* conformation. The two-dimensional structure is made of anionic double-sheet layers parallel to the *bc* plane, and K^+ and non-coordinated water molecules situated between the layers, as shown in Fig. 10. Each sheet is a kind of grid in the *bc* plane made of edge-sharing lozenges $[MoCNMn2NC]_2$. Two parallel sheets of a layer are further connected by $Mn1(CN)_4(H_2O)_2$ units situated between the sheets. The thickness of a double-sheet layer is 8.042 Å, and that of the gap between two layers is 7.263 Å.

Magnetic phase diagram

We first checked that *a*, *b* and *c** were the magnetic axes of the compound, *b* being the easy magnetization axis, then we studied the temperature and field dependences of the magnetization along the three axes. No hysteresis was observed along *a* and *b*, while a narrow hysteresis, of *ca.* 125 Oe, was observed along *c** at 5 K. These measurements revealed that the compound exhibits a long range ferromagnetic ordering at T_c = 39 K, and that below T_c a field induced spin reorientation occurs along the *c** axis. We determined the critical and saturation fields every 5 K below T_c when applying the field along *c**. The H_c and H_{sat} *versus T* curves shown in Fig. 11 define the magnetic phase diagram for the compound when the magnetic field is applied along *c**. This diagram is simpler than that of Fig. 7. It presents only three domains. Domain I corresponds to the paramagnetic, or saturated paramagnetic domain. Domain II corresponds to

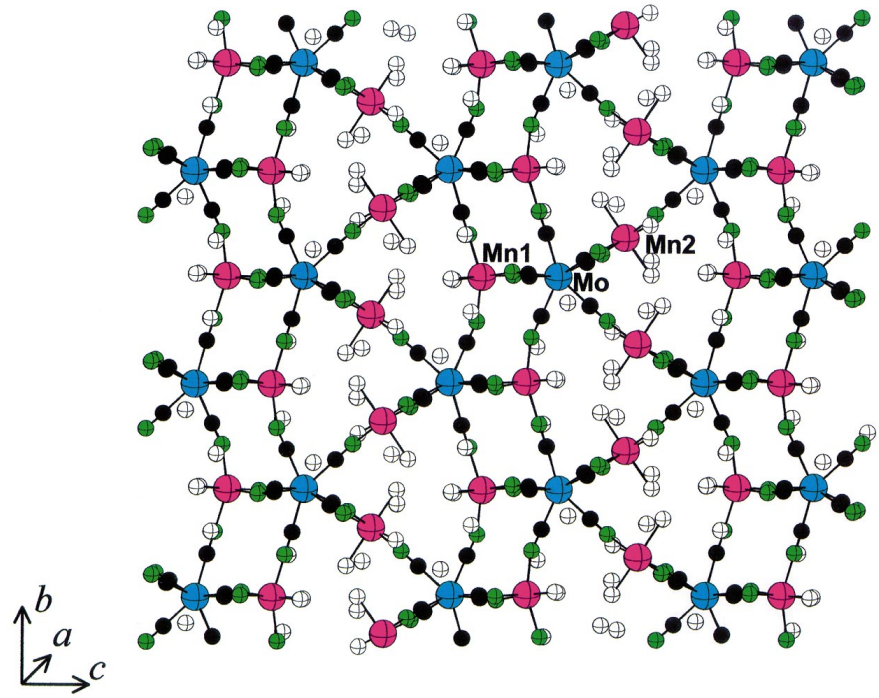

Fig. 8 Structure of the compound $Mn_2(H_2O)_5Mo(CN)_7{\cdot}4.75H_2O$ (β phase) viewed along the *a* direction.

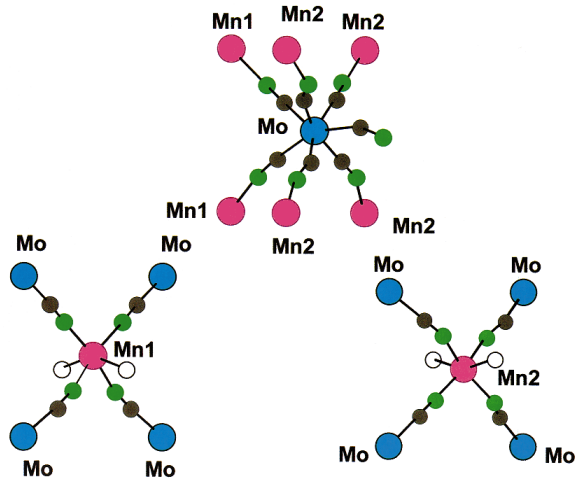

Fig. 9 Local structure of the molybdenum and manganese sites for $K_2Mn_3(H_2O)_6[Mo(CN)_7]_2{\cdot}6H_2O$. The color code is the same as for Fig. 1.

the ferromagnetically ordered domain in which the spins are essentially aligned along the *b* axis. Domain III, finally, is a spin-reorientation domain in which the spins rotate from the *b* to the *c** direction as the field increases from H_c to H_{sat}.

To complete this study, we also determined the temperature dependence of the spontaneous magnetization. For that, we studied the field dependence of the magnetization along the *b* axis every 5 K. Some curves are shown in Fig. 12 (top). At each temperature, the spontaneous magnetization, M_S, can be determined by extrapolating down to zero the $M = f(H)$ data obtained in the field range where the variation is linear. The temperature dependence of the spontaneous magnetization is represented in Fig. 12 (bottom). The spontaneous magnetization is equal to 17 $N\beta$ at absolute zero, decreases as the temperature increases, and vanishes at T_c = 39 K.

ac Magnetic measurements

So far, we only spoke of magnetic measurements recorded in the dc mode; *i.e.* with a static external field. Additional information can be obtained by working in the ac mode.[47] The magnetic field is then expressed as:

$$H = H_0 + h \exp(i\omega t)$$

where H_0 is the static field, which may be taken as zero, h is the amplitude of the oscillating field, ω the frequency, and t the time. The ac susceptibility, χ_{ac}, is then equal to dM/dH. The ac magnetic susceptibility is determined from its two components, the in-phase (or real) component, χ'_{ac}, and the out-of-phase (or imaginary) component, χ''_{ac}. The in-phase susceptibility is an initial susceptibility with the same phase as the oscillating field. The out-of-phase susceptibility characterizes the phase delay of the magnetization with respect to the oscillating field in the magnetically ordered phase.

We report here on two experiments in the ac mode. First, we measured the temperature dependences of the in-phase, χ'_{ac}, and out-of-phase, χ''_{ac}, magnetic susceptibilities under a zero static field. Along the three directions, the in-phase responses exhibit a break at T_c = 39 K. The χ'_{ac} values along the *b* axis below T_c are much higher than along the other two directions. The out-of-phase response along the *b* axis is zero down to 39 K, then presents an abrupt break as T is lowered below this temperature, and reaches a maximum around 34 K. Along the other two directions, χ''_{ac} is negligibly weak down to 2 K.

When the field is applied along the easy magnetization axis, *b*, both the displacement of the domain walls and the rotation of the magnetic moments contribute to the ac magnetic response. On the other hand, when the field is applied along a hard magnetization axis, only the rotation of the magnetic moments contributes to the ac response.[48] In the present case, the very high response along *b* as compared to the responses along *a* and *c** indicates that the domain walls move very easily, which is in line with the quasi absence of hysteresis in the $M = f(H)$ curves.

The second experiment consisted of measuring the field dependence of χ'_{ac} along the *c** axis every 5 K in the magnetically ordered phase. The results are displayed in Fig. 13. At each temperature, χ'_{ac} first increases as the field increases, reaches a maximum, then tends to zero at high field. The maximum of χ'_{ac} determines the critical field, H_c, and the extreme of the derivative $d\chi'_{ac}/dH$ determines the saturation field, H_{sat}. The $H_c = f(T)$ and $H_{sat} = f(T)$ curves deduced from this experiment are strictly similar to those shown in Fig. 11.

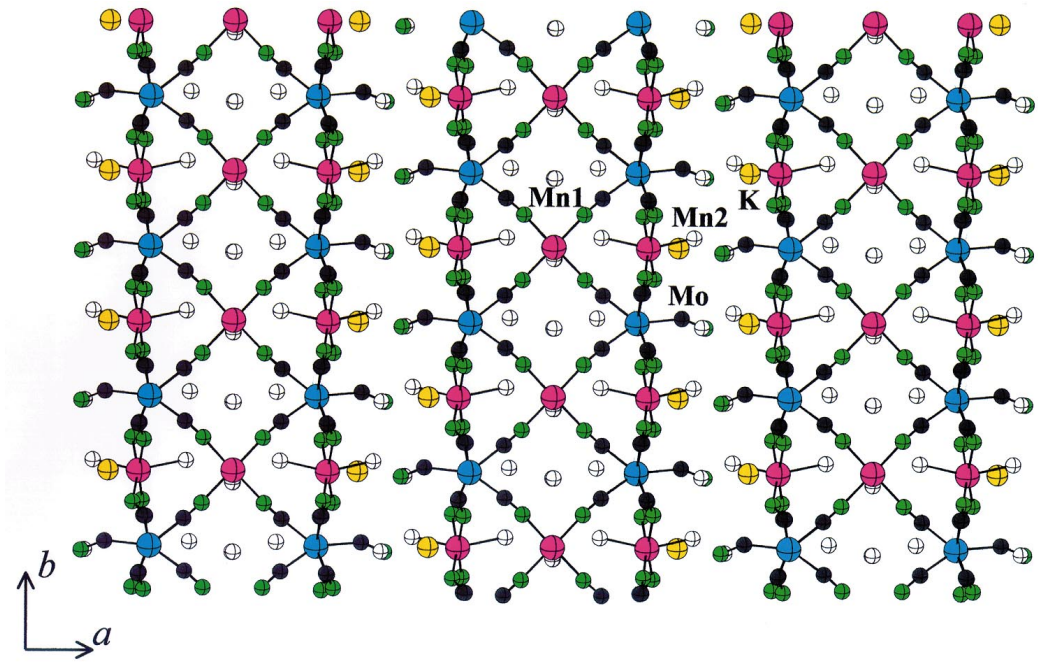

Fig. 10 Structure of the compound $K_2Mn_3(H_2O)_6[Mo(CN)_7]_2{\cdot}6H_2O$ in the *ab* plane. Potassium atoms are in yellow.

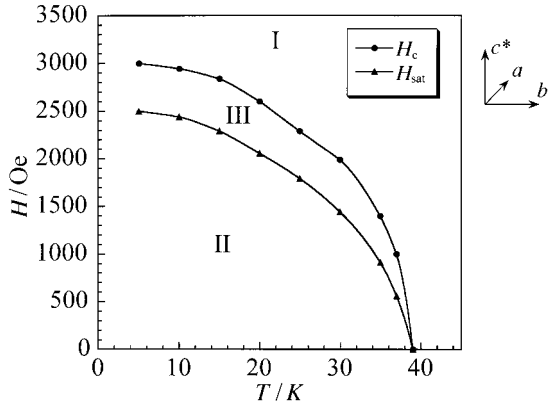

Fig. 11 Magnetic phase diagram for $K_2Mn_3(H_2O)_6[Mo(CN)_7]_2{\cdot}6H_2O$; the full lines are a guide to the eye.

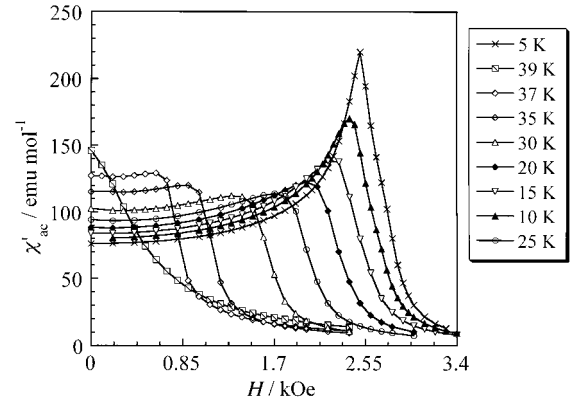

Fig. 13 Field dependences of the in-phase ac susceptibilities at different temperatures along the *c** axis for $K_2Mn_3(H_2O)_6[Mo(CN)_7]_2{\cdot}6H_2O$.

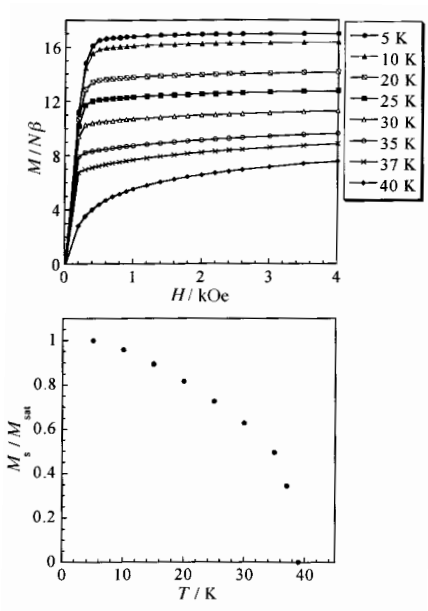

Fig. 12 (Top) Field dependences of the magnetization along the *b* axis at different temperatures for $K_2Mn_3(H_2O)_6[Mo(CN)_7]_2{\cdot}6H_2O$. (Bottom) Temperature dependence of the normalized spontaneous magnetization.

Modification of the magnetic properties through partial dehydration

The magnetic properties of $K_2Mn_3(H_2O)_6[Mo(CN)_7]_2{\cdot}6H_2O$ can be dramatically modified through partial dehydration. When the non-coordinated water molecules of a single crystal are released under vacuum, the external shape of the crystal is not modified. Magnetic measurements suggest that the crystallographic directions are retained. We then investigated the temperature dependences of the magnetization along these directions. The $M = f(T)$ curves along *b* and *c** are not distinguishable. After dehydration, the *bc* plane may be considered as an easy magnetization plane, even in low field. The spin reorientation is suppressed. Both in the *bc* plane and perpendicularly to this plane, the magnetization shows a break at T_c = 72 K, while the critical temperature for the non-dehydrated compound is 39 K. We measured the field dependences of the magnetization at 10 K both in the *bc** plane and along the *a* direction. The results are displayed in Fig. 14. In the easy magnetization plane, the saturation value of 17 $N\beta$ corresponding to the parallel alignment of all the spins is obtained under *ca.* 5.0 kOe. On the other hand, along the *a* axis, the saturation is not reached yet under 50 kOe. Magnetic hystereses are observed along both directions, with coercive fields of 1.3 kOe in the *bc* plane, and 0.55 kOe along *a*.

We can notice here that the Prussian blue phases are also hydrated. It would be interesting to see whether their partial dehydration also modifies their magnetic properties.

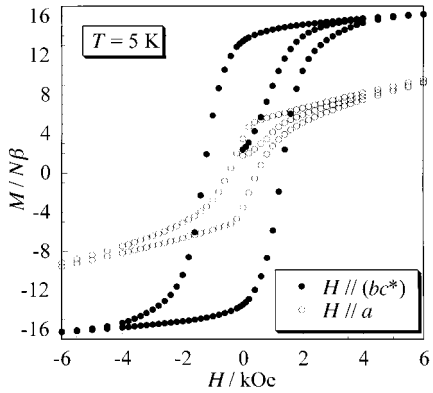

Fig. 14 Hysteresis loops in the *bc** plane and along the *a* axis at 10 K for a partially dehydrated crystal of $K_2Mn_3(H_2O)_6[Mo(CN)_7]_2{\cdot}6H_2O$.

Why is the Mo^{III}–C–N–Mn^{II} interaction ferromagnetic?

One of the striking features concerning the compounds described in this article is the ferromagnetic nature of the interaction between low-spin Mo^{III} and high-spin Mn^{II} ions through the cyano bridge. For several decades, quite a few studies have been devoted to the microscopic mechanisms of the interaction between spin carriers, more particularly to those of the mechanisms favoring a parallel alignment of the electron spins.[31,49] Three situations have been found to stabilize the parallel spin state, namely: (i) *the strict orthogonality of the magnetic orbitals*. Such a situation is achieved when all the singly occupied orbitals centered on a spin carrier (called also magnetic orbitals) are orthogonal (*i.e.* give a zero overlap integral) with all the singly occupied orbitals centered on the adjacent spin carrier. This situation of strict orthogonality of the magnetic orbitals is certainly the most efficient way to achieve a ferromagnetic interaction. (ii) *The electron transfer from a singly-occupied orbital on a site toward an empty orbital on an adjacent site, or from a doubly-occupied orbital on a site toward a singly-occupied orbital on an adjacent site*. This mechanism is probably less efficient than the previous one, and more difficult to control. (iii) *The interaction between a zone of negative spin density on a fragment and a zone of positive spin density on an adjacent fragment*. This mechanism, first suggested in the context of assemblies of organic radicals,[50] may apply for transition metal species as well.

We carefully examined the relevance of each of these mechanisms in the case of Mo^{III}–C–N–Mn^{II}. The strict orthogonality of the magnetic orbitals is not realized, and the absorption spectra of the compounds synthesized from the $[Mo(CN)_7]^{4-}$ precursor do not reveal any metal–metal charge transfer band of relatively low energy. Therefore, we are wondering whether the ferromagnetic interaction could arise from a close contact between negative and positive spin density zones.

The orbital energy diagram for low-spin Mo^{III} in pentagonal bipyramid symmetry (D_{5h}) is represented below.

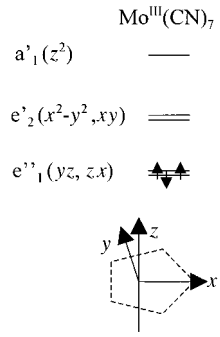

At the self consistent field (SCF) approximation, the e'_2 ($x^2 - y^2$, xy) and a'_1 (z^2) orbitals with a predominant 4d character are empty. It follows that at this approximation level, there is no spin density along both equatorial and axial Mo–C–N directions. It is now well established that such a view is oversimplified. The $^2E''_1$ SCF ground state may couple with SCF excited states of the same symmetry in which electrons have been promoted from the doubly-occupied and bonding e'_2 and a'_1 orbitals with a predominant cyano character to the empty and antibonding e'_2 and a'_1 orbitals with a predominant metal character. This configuration interaction gives rise to a negative spin density in the σ orbitals of the cyano ligands, along the Mo–C–N directions. This spin polarization effect has been experimentally observed in the hexacyanometallates involving 3d ions, such as $[Cr(CN)_6]^{3-}$ and $[Fe(CN)_6]^{3-}$, from polarized neutron diffraction experiments.[51,52]

The crucial point is that the stronger (*i.e.* the more covalent) the M–(CN) bond is, the more pronounced the spin polarization. Owing to the diffuseness of the 4d orbitals as compared to the 3d orbitals, the Mo^{III}–(CN) bond is significantly stronger than the Cr^{III}–(CN) or Fe^{III}–(CN) bond. It follows that the negative spin density along the Mo–C–N directions of the $Mo(CN)_7$ fragment might be particularly important. If it was so, the interaction between this negative spin density with a σ character and the σ singly occupied orbitals of Mn^{II} might favor the parallel alignment of the S_{Mo} and S_{Mn} spins.

If the interpretation above was correct, this would mean that the Mo^{III}–C–N–M interaction should be ferromagnetic for all M ions with unpaired electrons in σ (*i.e.* e_g in the case where M is in an octahedral environment) orbitals. All the data available so far confirm this idea.

What is the origin of the anisotropy?

Let us list the various factors affording magnetic anisotropy. We begin with the two local factors: the anisotropy of the ***g*** tensors and the zero-field splitting of the local spin states for the magnetic ions with a local spin higher than 1/2. In addition, there are several many-body (or collective) factors. These are: (i) the anisotropic interactions, resulting from the synergistic effect of the local spin–orbit coupling for an ion and the interaction between the excited states of this ion and the ground state of the adjacent ion; (ii) the antisymmetric interaction whose origin is similar to that of the anisotropic interaction, but in addition requires a low lattice symmetry; (iii) the dipolar interactions which may become important for lattices of low symmetry, and/or for high local spins (for instance $S_{Mn} = 5/2$); (iv) the shape anisotropy, finally, depending on the shape and size of the single crystals or particles utilized for the magnetic measurements.[38,53] Applying an external field H along the easy magnetization axis results in an internal field H_i related to H through:

$$H_i = H - NM$$

where N is the demagnetizing factor depending on the shape anisotropy, and NM the demagnetizing field. The field dependences of M shown in Fig. 6 are not corrected for the demagnetizing field.

Except when all the local spins are 1/2, the local zero-field splittings are usually more important than the anisotropic interactions. As for the antisymmetric interaction, it leads to spin canting, which may superimpose to both a ferromagnetic or an antiferromagnetic state. In this latter case, it gives rise to the phenomenon of weak ferromagnetism.[31]

What are the relevant factors in the case of the compounds described in this article? Mn^{II} in octahedral surroundings has a $^6A_1$ ground state, with a very weak zero-field splting. On the other hand, the ***g*** tensor for the $[Mo^{III}(CN)_7]$ chromophore is expected to be strongly anisotropic.[34] In other respects, the lattice symmetries are very low, even for the three-dimensional compounds. It follows that the two main anisotropy factors are the anisotropy of the ***g*** tensor for the $[Mo^{III}(CN)_7]$ chromophore along with the dipolar interactions. The spin reorientation might be due to a competition between these two factors. In zero (or low) external field, the ferromagnetically coupled local spins tend to align along the direction of the Mo–C–N–Mn–C–N

infinite linkages (for instance, the *b* axis for $Mn_2(H_2O)_5$-$Mo(CN)_7{\cdot}4H_2O$, α phase), which minimizes the dipolar energy. When the magnetic field reaches a certain value, the ***g*** anisotropy for Mo^{III} favors the spin alignment along another direction.

Conclusion

One of the peculiarities of molecular chemistry as compared to high-temperature solid state chemistry is that it usually affords species of low symmetry. In the field of molecule-based magnets, this low symmetry may lead to very interesting physical phenomena. Of course, the thorough investigation of these phenomena and their correct interpretation requires work on single crystals, which is time consuming and sometimes not trivial. However, accepting to do so may be very rewarding. To the best of our knowledge, the spin reorientation phenomenon had only been found so far for ferromagnetic intermetallic compounds, and not for insulating ferromagnets. In other respects, the magnetic phase diagrams of Fig. 7 and 11 are the very first for magnetic materials synthesized from molecular precursors.

The field of molecule-based magnets has many fascinating issues, such as strong coercivity, high critical temperature, processability, and photomagnetic effects.[54] The characterization of new phenomena arising from structural and magnetic anisotropies may be also considered as one of these issues.

Acknowledgements

This work was partly funded by the TMR Research Network ERBFMRXCT980181 of the European Union, entitled: Molecular Magnetism; from Materials toward Devices.

References

1 J. S. Miller, J. C. Calabrese, A. J. Epstein, R. W. Bigelow, J. H. Zang and W. M. Reiff, *J. Chem. Soc., Chem. Commun.*, 1986, 1026.
2 Y. Pei, M. Verdaguer, O. Kahn, J. Sletten and J.-P. Renard, *J. Am. Chem. Soc.*, 1986, **108**, 428.
3 J. S. Miller, J. C. Calabrese, H. Rommelman, S. R. Chittipedi, J. H. Zang, W. M. Reiff and A. J. Epstein, *J. Am. Chem. Soc.*, 1987, **109**, 769.
4 O. Kahn, Y. Pei, M. Verdaguer, J.-P. Renard and J. Sletten, *J. Am. Chem. Soc.*, 1988, **110**, 782.
5 A. Caneschi, D. Gatteschi, R. Sessoli and P. Rey, *Acc. Chem. Res.*, 1989, **22**, 392.
6 W. E. Broderick, J. A. Thompson, E. P. Day and B. M. Hoffman, *Science*, 1990, **249**, 410.
7 G. T. Yee, J. M. Manriquez, D. A. Dixon, R. S. McLean, D. M. Groski, R. B. Flippen, K. S. Narayan, A. J. Epstein and J. S. Miller, *Adv. Mater.*, 1991, **3**, 309.
8 Y. Nakazawa, M. Tamura, N. Shirakawa, D. Shiomi, M. Takahashi, M. Kinoshita and M. Ishikawa, *Phys. Rev. B*, 1992, **46**, 8906.
9 H. Tamaki, Z. J. Zhong, N. Matsumoto, S. Kida, S. Koikawa, S. Achiwa, Y. Hashimoto and H. Okawa, *J. Am. Chem. Soc.*, 1992, **114**, 6974.
10 R. Chiarelli, M. A. Nowak, A. Rassat and J.-L. Tholence, *Nature*, 1993, **363**, 147.
11 J. S. Miller and A. J. Epstein, *Angew. Chem., Int. Ed. Engl.*, 1994, **33**, 385.
12 D. Gatteschi, *Adv. Mater.*, 1994, **6**, 635.
13 K. Inoue and H. Iwamura, *J. Am. Chem. Soc.*, 1994, **116**, 3173.
14 S. Decurtins, H. W. Schmalle, H. R. Oswald, A. Linden, J. Ensling, P. Gütlich and A. Hauser, *Inorg. Chim. Acta*, 1994, **216**, 65.
15 S. Descurtins, H. W. Schmalle, P. Schneuwly, J. Ensling and P. Gütlich, *J. Am. Chem. Soc.*, 1994, **116**, 9521.
16 M. Ohba, N. Maruono and H. Okawa, *J. Am. Chem. Soc.*, 1994, **116**, 11566.
17 K. Inoue, T. Hayamizu, H. Iwamura, D. Hashizume and Y. Ohashi, *J. Am. Chem. Soc.*, 1996, **118**, 1803.
18 C. Mathonière, C. J. Nuttall, S. Carling and P. Day, *Inorg. Chem.*, 1996, **35**, 1201.
19 H. Iwamura, K. Inoue and N. Koga, *New J. Chem.*, 1998, **10**, 201.
20 H. O. Stumpf, L. Ouahab, Y. Pei, D. Grandjean and O. Kahn, *Science*, 1993, **261**, 447.
21 H. O. Stumpf, L. Ouahab, Y. Pei, P. Bergerat and O. Kahn, *J. Am. Chem. Soc.*, 1994, **116**, 3866.
22 M. G. F. Vaz, L. M. M. Pinheiro, H. O. Stumpf, A. F. C. Alcântara, S. Gohlen, L. Ouahab, O. Cador, C. Mathonière and O. Kahn, *Chem. Eur. J.*, in press.
23 S. Ferlay, T. Mallah, R. Ouahès, P. Veillet and M. Verdaguer, *Nature*, 1995, **378**, 701.
24 A. Ludi and H. Güdel, *Struct. Bonding* (*Berlin*), 1973, **14**, 1.
25 O. Kahn, *Adv. Inorg. Chem.*, 1995, **43**, 179.
26 D. Babel, *Comments Inorg. Chem.*, 1986, **5**, 285.
27 V. Gadet, T. Mallah, I. Castro and M. Verdaguer, *J. Am. Chem. Soc.*, 1992, **114**, 9213.
28 T. Mallah, S. Thiebaut, M. Verdaguer and P. Veillet, *Science*, 1993, **262**, 1554.
29 W. R. Entley and G. S. Girolami, *Inorg. Chem.*, 1994, **33**, 5165.
30 W. R. Entley and G. S. Girolami, *Science*, 1995, **268**, 397.
31 O. Kahn, *Molecular Magnetism*, VCH, New York, 1993.
32 O. Kahn, *Nature*, 1995, **378**, 667.
33 G. R. Rossman, F. D. Tsay and H. B. Gray, *Inorg. Chem.*, 1973, **12**, 824.
34 M. B. Hursthouse, K. M. A. Maijk, A. M. Soares, J. F. Gibson and W. P. Griffith, *Inorg. Chim. Acta*, 1980, **45**, L81.
35 R. C. Young, *J. Am. Chem. Soc.*, 1932, **54**, 1402.
36 J. Larionova, J. Sanchiz, S. Golhen, L. Ouahab and O. Kahn, *Chem. Commun.*, 1998, 953.
37 J. Larionova, R. Clérac, J. Sanchiz, O. Kahn, S. Golhen and L. Ouahab, *J. Am. Chem. Soc.*, 1998, **120**, 13088.
38 W. A. Wooster, *Tensor and Group Theory for the Physical Properties of Crystals*, Clarendon Press, Oxford, 1973.
39 A. K. Gregson and N. T. Noxon, *Inorg. Chem.*, 1982, **21**, 3464.
40 M. A. Salgueiro da Siva, J. M. Moreira, J. A. Mendes, V. S. Amaral, J. B. Sousa and S. B. Palmer, *J. Phys.: Condens. Mater.*, 1995, **7**, 9853.
41 B. Garcia-Landa, E. Tomey, D. Fruchart, D. Gignoux and R. Skolozdra, *J. Magn. Magn. Mater.*, 1996, **157–158**, 21.
42 W. A. Mendoza and S. A. Shaheen, *J. Appl. Phys.*, 1996, **79**, 6327.
43 G. Cao, S. McCall and J. E. Crow, *Phys. Rev. B*, 1997, **55**, R672.
44 X. C. Kou, M. Dahlgren, R. Grössinger and G. Wiesinger, *J. Appl. Phys.*, 1997, **81**, 4428.
45 J. Larionova, O. Kahn, S. Golhen, L. Ouahab and R. Clérac, *Inorg. Chem.*, in press.
46 J. Larionova, O. Kahn, S. Gohlen, L. Ouahab and R. Clérac, *J. Am. Chem. Soc.*, in press.
47 F. Palacio, F. J. Lazaro and A. J. Duyneveldt, *Mol. Cryst. Liq. Cryst.*, 1989, **176**, 289.
48 X. C. Kou, R. Grössinger, G. Hischer and H. R. Kirchmayr, *Phys. Rev. B*, 1996, **54**, 6421.
49 C. Kollmar and O. Kahn, *Acc. Chem. Res.*, 1993, **26**, 259.
50 H. M. McConnell, *J. Chem. Phys.*, 1963, **39**, 1910.
51 B. N. Figgis, J. B. Forsyth and P. A. Reynolds, *Inorg. Chem.*, 1987, **26**, 101.
52 B. N. Figgis, E. S. Kucharski and M. Vrtis, *J. Am. Chem. Soc.*, 1993, **115**, 176.
53 A. Bencini and D. Gatteschi, *EPR of Exchange Coupled Systems*, Springer-Verlag, Berlin, Germany, 1989.
54 O. Sato, T. Iyoda, A. Fujishima and K. Hashimoto, *Science*, 1996, **272**, 704.

Paper 9/00180H